Comparative study on the support properties in the total oxidation of dichloromethane over Pt catalysts

Zouhair El Assal, Satu Ojala, Satu Pitkäaho, Laurence Pirault-Roy, Bouchra Darif, Jean-Dominique Comparot, Mohammed Bensitel, Riitta L. Keiski, Rachid Brahmi

Comparative study on the support properties in the total oxidation of dichloromethane over Pt catalysts

Zouhair El Assal, Satu Ojala, Satu Pitkäaho, Laurence Pirault-Roy, Bouchra Darif, Jean-Dominique Comparot, Mohammed Bensitel, Riitta L. Keiski, Rachid Brahmi

PII: S1385-8947(16)31548-0
DOI: http://dx.doi.org/10.1016/j.cej.2016.10.139
Reference: CEJ 15995

To appear in: *Chemical Engineering Journal*

Received Date: 18 July 2016
Revised Date: 28 September 2016
Accepted Date: 31 October 2016

Please cite this article as: Z. El Assal, S. Ojala, S. Pitkäaho, L. Pirault-Roy, B. Darif, J-D. Comparot, M. Bensitel, R.L. Keiski, R. Brahmi, Comparative study on the support properties in the total oxidation of dichloromethane over Pt catalysts, *Chemical Engineering Journal* (2016), doi: http://dx.doi.org/10.1016/j.cej.2016.10.139

Comparative study on the support properties in the total oxidation of dichloromethane over Pt catalysts

Zouhair El Assal[1,2,3], Satu Ojala[1], Satu Pitkäaho[1], Laurence Pirault-Roy[4], Bouchra Darif[1,3], Jean-Dominique Comparot[4], Mohammed Bensitel[3], Riitta L. Keiski[1*] and Rachid Brahmi[3]

[1]Environmental and Chemical Engineering, Faculty of Technology, P.O. Box 4300, FI-90014 University of Oulu, Finland

[2]Thule institute P.O. Box 7300, FI-90014 University of Oulu, Finland

[3]Laboratory of Catalysis and Corrosion of Materials (LCCM), Department of Chemistry, Faculty of Sciences of El Jadida, University of Chouaïb Doukkali, BP.20, 24000 El Jadida, Morocco

[4]Institute of Chemistry of Poitiers: materials and natural resources, IC2MP-UMR 7285, University of Poitiers, B27, 4, Rue Michel Brunet, TSA 51106- 86073 Poitiers Cedex France

* Correspondence: riitta.keiski@oulu.fi; Tel.: +358294482348

Abstract

The aim of this work was to study the influence of the support oxide properties on the total oxidation of dichloromethane in moist conditions. The support materials γ-Al_2O_3, TiO_2, CeO_2 and MgO were synthesized by a sol-gel method followed by wet impregnation of Pt and characterized by different physico-chemical techniques. The conversion of DCM was higher than 90% at 500 °C over impregnated and non-impregnated Al_2O_3, TiO_2 and CeO_2, even at high GHSV. CO, CH_3Cl and CH_2O were the major by-products observed and their amounts decreased after Pt impregnation. The CH_3Cl formation was higher when Lewis acid sites were present while the existence of Brønsted sites promoted the CH_2O formation. The complete conversion of DCM was achieved at around 450 °C over the Al_2O_3 and Pt/Al_2O_3 and at 500°C for Pt/TiO_2. These two catalysts exhibited the highest total acidities among the materials tested. The activity of Pt/Al_2O_3 remained the same also after 55 h of testing, however, increase in Pt particle size and decrease in acidity were observed. Pt/CeO_2 while being less active showed smallest amount of by-product formation during the whole temperature range used in light-off tests. This is most probably due to its easy reduction ability. The textural parameters of the supports did not appear to be the key parameters when considering the activity and selectivity of the catalysts.

Keywords:

Brønsted acidity; catalytic oxidation; CVOC abatement; dichloromethane; Lewis acidity; methyl chloride

1. Introduction

Dichloromethane (methylene chloride, CH_2Cl_2, DCM) is widely used in industry in paint strippers and removers, as propellants in aerosols, in the manufacture of drugs, decaffeination of coffee etc. [1,2]. Majority of DCM detected in the environment is due to human actions. However, DCM is not very persistent in the environment. It is quite easily photochemically oxidised by hydroxyl radicals and it does not contribute significantly to the ozone depletion nor to the photochemical smog formation [3]. The volatility increases the health effects of DCM due to facility of inhalation. Long contact with DCM causes problems with skin, central nervous system and liver. Even deaths of the employees are reported to be caused by use of DCM in US [8]. DCM is also considered as a human carcinogen. [4] Several authorities have set the exposure limits for the DCM, which are for example in Europe, 100 ppm (8h) and 200 ppm (15 min) [5].

Catalytic oxidation is an economic and environmentally sound abatement method, since it is effective in destroying even diluted streams of volatile organic compounds (VOCs) as well as chlorinated volatile organic compounds (CVOCs) at a low temperature range (200-500°C) [6]. In addition, CVOC oxidation in the presence of efficient catalysts leads selectively to the desired reaction products CO_2, H_2O and HCl, and the harmful and toxic by-products such as dioxins can be avoided [7]. DCM is one of most frequently used model compound for CVOCs, since it constitutes a significant fraction of CVOCs' industrial emissions. [8–15]

Different noble metals (Pd, Pt, Rh) supported on various metal oxides such as Al_2O_3, TiO_2, MgO and CeO_2 alone or as mixed oxides are mostly studied catalysts in CVOC oxidation. Brink *et al.* [16] have studied DCM oxidation over γ- Al_2O_3. During the DCM oxidation, they observed CO and CH_3Cl as the major by-products in addition to HCl. Padilla *et al.* [8] and Corella *et al.* [9] studied various CVOCs, including DCM, over different aluminium and titanium oxides and shaped (monoliths, sphere,

pellet) catalysts containing Cu, Cr, Pt and Pd. They obtained higher than 80% conversion of DCM with the formation of $CHCl_3$ and CCl_4 as the major by-products. They also observed that Pt based catalysts are more active than the other metal based catalysts studied. Pitkäaho *et al.* [10] studied γ-alumina supported Pt, Pd, Rh and V_2O_5 monolith catalysts. The formation of CH_2O, CO and CH_3Cl was seen to decrease when platinum and /or ceria was added to the catalyst. Pt/Al_2O_3 was found to be the most active and selective catalyst: 100% conversion was reached at 420 °C and the HCl yield detected was 92%.

Pinard *et al.* [11,12] and Maupin *et al*. [13] investigated the DCM oxidation over different zeolite (NaY, HFAU and FAU) and alumina (Al_2O_3 and Pt/Al_2O_3) based catalysts. They concluded that the first step of DCM conversion occurs on the support in the presence of steam with the formation of by-products, the nature and quantity of which depend on the nature of the acidic sites present on the support surface: CH_3Cl is formed on the Lewis acid sites (LAS) whereas CH_2O is formed on the Brønsted acid sites (BAS). Then, these by-products are transformed to final products (HCl and CO_2) on the noble metal sites (Pt). Wang *et al.* [17] studied the oxidation of DCM over a platinum catalyst supported on an anodic alumite plate. They also observed the formation of by-products, the amount of which decreased with the addition of Pt on the surface of the support.

Based on the earlier studies, it seems that the support properties have a crucial role in the initiation of the DCM reaction on the catalyst. In this study, we selected four different types of supports to compare their properties in more detail. Al_2O_3, having both Lewis and Brønsted acid sites on its surface, was selected to represent acidic support. The good activity of MgO in CCl_4 conversion and its interesting selectivity towards HCl and CO_2 formation were pointed out earlier by Weiss *et al.* [18]. This is why we decided to choose MgO as a material representing basic properties. Furthermore, a good oxygen storage and oxygen activator [19–21], CeO_2, was selected to check the effect of improved oxidation properties of the support material. TiO_2 was studied as it has shown good selectivity towards

H_2O, CO_2 and Cl_2 formation and high stability [22]. To summarize, four oxides Al_2O_3, TiO_2, MgO and CeO_2, with and without Pt impregnation, representing different acido-basic and physico-chemical properties were characterized and tested in DCM oxidation aiming at to find out more information on the role of the support in DCM oxidation.

2. Materials and Methods

2.1. Catalyst preparation

The γ-Al_2O_3 support was prepared from aluminium-tri-sec-butoxide (AB, $Al(O\text{-}C_4H_9)_3$, Sigma-Aldrich, 97 wt-%) precursor using a sol-gel method proposed by Yoldas [23]. The molar ratio of 1:100:0.1 for AB:H_2O:HCl was used in the preparation. The mixture of AB and ultrapure water were kept under stirring at 60°C for 60 min followed by the addition of HCl in order to catalyse the condensation process. Then, the mixture was kept at 80 °C under vigorous stirring for 2 h after which a viscous sol was obtained. During the preparation, the beaker was covered to minimize evaporation of water.

The preparation of TiO_2, CeO_2 and MgO supports is described in detail in our previous study [24]. Briefly, it consists of a sol-gel preparation using alkoxide precursors for titanium and magnesium and an ionic salt for cerium (cerium (III) nitrate hexahydrate). In the preparation, the precursors were dissolved in alcohol and after water addition the sol-gel formation occurs.

All the prepared viscous sols were dried on a sand bath at 60 °C (formation of gel during drying) overnight followed by drying in a ventilated oven at 120 °C, and finally calcined at 500 °C for 6 hours after the temperature had been increased from room temperature to the final calcination temperature with the heating rate of 5 °C min^{-1}.

The hexachloroplatinic acid ($H_2PtCl_6 \cdot xH_2O$, Johnson-Mattey, 99.9%) was used as a precursor of platinum in wet impregnation to obtain 0.5 wt-% of metallic platinum on the final catalyst. The precursor solution was mixed with the support and maintained under mechanical stirring overnight and then dried at 60 °C on a sand bath. The catalysts were calcined at 500 °C for 2 h followed by a reduction step under a hydrogen flow diluted in N_2 (1/3 H_2 and 2/3 N_2) at 500 °C for 2 h. Heating rate used in both cases was 5°C min^{-1}. PtAl, PtTi, PtCe and PtMg are used as acronyms for the impregnated catalysts, i.e. Pt/γ-Al_2O_3, Pt/TiO_2, Pt/CeO_2, Pt/MgO, respectively.

2.2. Catalyst characterization

TGA and DTA curves of the non-calcined supports were obtained using SDT2960 TA and SDTQ600 analyzers. Prior to experiments the samples were dried at 120 °C after which they were packed into a Pt crucible. The weights of the samples were between 20 to 30 mg. Samples were analysed in the temperature range of 25 to 1000 °C with a heating rate of 10 °C min^{-1} under an air flow (100 mL min^{-1}). The information achieved was used in the selection of the correct calcination temperature for the supports.

XRD data were collected at room temperature, using a Bruker D8 diffractometer, equipped with a Cu Kα radiation ($\lambda K_{\alpha 1}$ = 0.15406 nm) anode X-ray tube and Nickel filter monochromator. Diffractograms were recorded in the 5–90° range of 2θ with a step of 0.05° and a dwell time of 2 s. For sample identification, diffraction patterns were compared to the JCPDS database (Joint committee on powder diffraction standards). The crystallite sizes were calculated using the Debye–Scherrer equation (1):

$$D = k\lambda/(\beta\cos\theta) \qquad (1)$$

were θ (°) is the Bragg angle, D (Å) is the average crystallite size, k = 0.94 and β (°) the corrected FWHM, after correction of the broadening coming from the instrument, which is evaluated from the LaB_6 standard as described in [24].

The samples were characterized using nitrogen physisorption, the specific surface area was estimated by the BET method and the mean pore size diameter by the BJH method. The data were obtained from the N_2 adsorption–desorption isotherms at -196 °C, using an ASAP 2020 apparatus. Before the analysis, the samples were outgassed at 350 °C for 2 h.

Elemental analysis using inductively coupled plasma atomic emission spectroscopy (ICP-AES) technique, performed on a Perkin Elmer Optima 2000 DV apparatus, was used to determine the content of Pt present on the catalysts.

Transmission Electron Microscopy analysis was done using a TEM/STEM JEOL 2100 UHR 0.19 nm resolution, equipped with an energy dispersive spectrometer EDX and High-Angle Annular Dark-Field HAADF. The particle size distribution was obtained from the TEM images and the average particle diameter (dp) was calculated using the following equation (2):

$$dp = \sum n_i d_i^3 / \sum n_i d_i^2 \qquad (2)$$

where n_i is the number of particles with the size d_i.

Temperature Programmed Reduction experiments (TPR) were performed with a Micromeritics AutoChem II 2920 device. Before analysis, the samples (~200 mg) were heated from RT to 500 °C in oxygen flow (50 mL min^{-1}) with the heating rate of 5 °C min^{-1} and keeping the samples at 500 °C for 60 min. The samples were then cooled down to RT under O_2 and outgassed under argon for 30 min. Finally TPR was performed from RT up to 500 °C with the heating rate of 5 °C min^{-1} and maintaining the final temperature for 10 min under diluted hydrogen flow (1% H_2 in Ar (100 mL min^{-1}) for

catalysts, and 10 % H_2 in Ar (50 mL min^{-1}) for supports). A Thermal Conductivity Detector (TCD) was used to quantify H_2 consumption.

The X-ray photoelectron spectroscopy (XPS) analyses for catalysts before and after the activity test were performed with a Thermo Fisher Scientific ESCALAB 250Xi X-ray photoelectron spectroscopy (XPS) system equipped with Al K_α X-ray source = 1486.7 eV to study the Cl amount on TiO_2 and CeO_2 based catalysts. The X-ray source operated at 10 mA and 12 kV. The spectral regions corresponding to Cl2p, Pt 4f, Ti2p, Ce3d and O1s core levels were recorded for each sample. The results were treated by Thermo Avantage V5.957 software by using Gaussian/Lorentzian curve fitting after removing the background by Shirley function. The static charge of the samples was corrected by referencing all binding energies (BE) of TiO_2 based catalysts to the C1s peak (285 eV). In the case of CeO_2 based catalysts, the Ce $3d_{3/2}$ peak at 916.8 eV was used for the correction of the spectra, since the intensity of the C1s peak was not adequate [25].

For total acidity measurements, temperature programmed desorption of ammonia (NH_3-TPD) was done with an AutoChem II 2920 device. Prior to the analysis, the sample (about 200 mg) was pre-treated from RT to 500 °C with 5 °C min^{-1} heating rate for 30 min, and then cooled down to RT under a He flow. The NH_3 adsorption (15% NH_3 in He flow of 50 mL min^{-1}) was done at room temperature during 60 min, after which the sample was flushed with He for 30 min. The NH_3 desorption was carried out from RT to 650 °C (5 °C min^{-1}) for all the supports and up to 500 °C for Pt containing catalysts. The concentration of desorbed NH_3 was analysed by a TCD detector. The total acidity of samples was determined by integration of the area between 50-500 °C.

For pyridine desorption, the procedure described in detail in [24] was used. The IR spectra were recorded *in-situ* during the pyridine desorption from the samples (a self-supporting wafer with a diameter of 16 mm) at different temperatures. Before recording the spectra, samples were evacuated for 20 min at each temperature (at room temperature, 50 °C and then with 50 °C steps to 450 °C).

Hereafter, only the wavenumber range from 1400 to 1700 cm^{-1} is discussed, since it contains all the important acid vibration bands when pyridine is used as a probe molecule [26].

Lutidine desorption was done nearly in the same way as the pyridine desorption, but with a small change. At the beginning of the measurement, 2 mbar of lutidine was adsorbed on the samples for 5 min, and before recording the spectra, samples were evacuated for 30 min at each temperature. The acid sites were calculated by using the average extinction coefficient obtained by Onfroy *et al.* [27].

2.3. Catalytic oxidation of dichloromethane

The DCM oxidation experiments were carried out in a tubular continuous flow reactor. Liquid DCM and water were fed with syringe pumps equipped with gas tight syringes to the evaporator and mixed with a controlled amount of air. The gas analysis was done with a Gasmet DX-4000N FTIR analyser, which was calibrated to detect the following chlorinated hydrocarbons: C_2Cl_4, C_2HCl_3, CH_3Cl, CH_2Cl_2, $CHCl_3$, $COCl_2$ and HCl in addition to CO, CO_2, CH_2O, CH_4 and C_2H_7OH. More details about the experimental set-up can be found from reference [28].

The DCM (Sigma Aldrich) concentration was 500 ppm in all the activity tests and the tests were performed in the presence of 1.5 vol-% of water to ensure the sufficient selectivity towards the HCl formation and to prevent catalyst deactivation [10,28]. The total gas flow was set to 1.02 L min^{-1} through the catalyst bed of 400 mg for all the other samples, except for the MgO, giving the GHSV of 143 790 h^{-1}. In the case of MgO the mass of 167 mg was used to keep the GHSV constant when the results are compared. Due to the smaller mass of MgO, a verification test was done with a sample of 400 mg giving GHSV of 52 600 h^{-1}. No significant differences between the two experiments were observed and lower amount of MgO giving the same GHSV with the other samples was used. The temperature range during the oxidation test was from 100 to 500 °C and the heating rate of 5 °C min^{-1}

was used. The experiments were always repeated at least once to verify the results. The DCM conversion (% DCM) and HCl yield (%Y) were calculated as follows:

$$\%\mathrm{DCM} = 100 \times (1 - \frac{C_{DCM}^{out}}{C_{DCM}^{in}}) \quad (3)$$

$$\%\mathrm{Y} = 100 \times \frac{C_{HCl}^{out}}{2 * C_{DCM}^{in}} \quad (4)$$

where C_{DCM}^{re} is the reacted DCM, C_{HCl}^{out} the outlet HCl concentration and C_{DCM}^{in} is the inlet DCM concentration.

Before the catalytic activity tests, a thermal oxidation test (HT, blank test) was done without a catalyst. In addition, a diffusion study was done over γ-Al_2O_3 to verify the mass transfer effects in the DCM conversion. Internal diffusion was studied by changing the particle size while keeping the other parameters unchanged, and external diffusion was studied by changing the mass of the sample and the gas flow rate to keep the GHSV constant. The diffusion study showed that the effect of internal diffusion should be taken into account, and thereafter we have chosen to use the fixed granule size with the diameter between 0.25 and 0.5 mm for all the samples. This selection allowed us to avoid too high pressure drop in the reactor caused by the catalyst packing.

In order to study the durability of the most active catalyst an extended test was done. This test started with a light-off test (between 100 and 500 °C) and then the temperature was fixed at 400 °C. After 55 h of testing a supplementary light-off test was done from 100 until 500 °C in order to make comparison of DCM conversion and products yield between the initial state and after the durability test.

3. Results and discussion

3.1. Characterization

After calcination of the prepared supports at 500°C, γ-Al_2O_3, anatase (TiO_2), periclase (MgO) and cerianite (CeO_2) were the identified phases based on the XRD analysis. Alumina support contained also

a significant amount of amorphous material. The γ-Al_2O_3 support presented the smallest crystallite size (around 4 nm) while other supports had crystallite sizes between 11 and 18 nm (Table 1). These results are in good correlation with the determined specific surface areas, since smaller crystallites lead to a higher S_{BET}.

Table 1. Textural and structural characterization results of the prepared materials, D_M: Approximate average size of crystallites determined by XRD, S_{BET}: Specific surface area, P_v: Pore volume, D_p: Average pores size, wt-% Pt: Mass of Pt determined by ICP, T_M: Average size of Pt particles determined by TEM and * mean S_{BET} of corresponding catalysts.

	Supports characterization				**Pt based Catalysts characterization**		
	D_M (nm)	**S_{BET} (m^2g^{-1})**	**P_v (cm^3g^{-1})**	**D_p (nm)**	**wt-% Pt**	**S^*_{BET} (m^2g^{-1})**	**T_M (nm)**
Al_2O_3	4	255	0.4	6	0.7	227	~1.2
CeO_2	11	89	0.3	13	0.6	82	~2.4
TiO_2	16	75	0.2	9	0.5	53	3.6
MgO	18	64	0.2	11	0.5	33	3.7

The nitrogen adsorption-desorption isotherms for all the supports fit into the Type IV according to the IUPAC classification indicating mesoporous materials. The measured average pore size of the supports is varying between 6-13 nm as shown in Table 1. [29] The ICP analysis revealed that the target amount of Pt (0.5 wt-%) was achieved quite well for the TiO_2 and MgO, but the Pt loading on CeO_2 and Al_2O_3 was slightly higher than expected (Table 1).

The results of temperature programmed reduction (H_2-TPR) over different catalysts and supports are shown in Fig. 1. The H_2-TPR curves for supports except CeO_2 do not exhibit significant consumption of H_2 in the temperature range of 50 to 500 °C. With TiO_2 we observe a minor H_2 consumption that starts after 400°C. For example Avila *et al.* [30] did not observe any reduction of TiO_2 when heating material up to 500°C under 5% H_2 flow. In the case of CeO_2, we observe a peak between 250 and 500

°C with the maximum at around 430 °C. This peak is corresponding to the reduction of surface Ce^{4+}. The same peak is also observed in the case of PtCe in the range of 310-500 °C with the maximum at around 380 °C (not visible in Figure 1.b due to the scale of the figure). The appearance of the peak maximum at lower temperature is due to the presence of Pt, which facilitates the Ce^{4+} reduction. [31,32] In addition, PtCe show a very strong H_2 consumption between 190-240°C. This peak is related to the reduction of Pt, since the non-impregnated supports do not show any reduction below 290°C after which the reduction of the surface Ce^{4+} starts [32,33]. As discussed later, this peak involves also ceria reduction via spill over from Pt based on the related H_2 consumption.

In the case of PtMg the strong peak (190-240°C) is accompanied with two smaller reduction peaks with the maxima at 280°C and 350°C. These may be related to Pt^{4+} reduction to Pt^{2+}, and also reduction of Pt^{2+} interacting with the support [34]. Due to the acidity of hexachloroplatinic acid used in impregnation, MgO may be partly dissolved and cause partial encapsulation of platinum. [34] This may affect also the reduction behaviour of the PtMg catalyst.

At low temperatures below 100 °C, a small consumption of H_2 is observed for all the catalysts. This is most probably due to metal particles that have low interaction with the surface of supports [35] and related to the reduction of PtOx as suggested by Reyes et al [36]. If we assume the existence of PtO on the catalysts, the consumption of H_2 at low temperature is able to reduce only less than 2% of Pt. When the total consumption of H_2 was calculated between 50 and 500°C for all the catalysts, it was observed that only in the case of PtCe the H_2 consumption is higher than the theoretical amount needed for the complete Pt^{2+} reduction, which means that reduction of CeO_2 occurs as well. Based on the results it seems that PtO_x was not completely reduced in the cases of MgO, Al_2O_3 and TiO_2 or it was not fully oxidized during the pre-treatment procedure.

TPR measurements may be affected by the slight differences in the loading of Pt on the different supports and the presence of residual Cl from the hexachloroplatinic acid. Chen *et al*. [37] proposed

that a smaller amount of Pt has better interaction with CeO_2 and therefore facilitates the reduction of the catalyst. However, they did not consider the possible effect of residual chlorine from the precursor salt. Hwang *et al*. [38] show that the reduction of Pt-O_x occurs at lower temperature (<150°C) than the reduction of PtO_xCl_y (150-400°C) and the presence of PtO_xCl_y inhibits the reduction of the platinum ions. They propose the removal of these complexes by reduction at 400°C. They used $PtCl_4$ as the Pt precursor and the support used was Al_2O_3. In our case, the catalysts were reduced at 500°C for 2 h during the preparation.

Fig. 1

The TEM images (Fig. 2) show that Pt was rather homogenously distributed on the supports as nanoparticles. The Pt particle size distribution indicated about 1 nm average size for Pt particles on Al_2O_3. Other samples present particles with average sizes from 2 to 4 nm. However, some significantly larger particles are also observed in the cases of PtTi and PtMg. The existence of different particle sizes could explain the existence of several reduction peaks in TPR analysis in addition to interactions of the metal particles with the support. According to earlier findings, larger particles would decrease the observed reduction temperatures [35].

Fig. 2

3.2. Acidity measurements

The NH_3-TPD analysis performed on different catalysts is shown in Fig. 3. According to the figure, PtAl and PtTi have more medium strength acid sites than PtCe and PtMg. The total amounts of acid

sites of catalysts (determined between 50-500 °C) are shown in Table 2 calculated for the mass of the catalyst and taking into account the specific surface area of the material.

Table 2. Total acidity of the materials based on NH_3-TPD determined between 50-500°C.

50-500°C	PtAl	Al_2O_3	PtTi	TiO_2	PtCe	CeO_2	PtMg	MgO	θ-Al_2O_3	α-Al_2O_3
µmol g^{-1}	189	156	79	74	60	49	21	18	75	20
µmol m^{-2}	0.83	0.61	1.49	0.98	0.73	0.55	0.64	0.28	0.63	0.17

The table shows that alumina and titania based catalysts have more acid sites than ceria and magnesia based catalysts. The amount of acid sites per gram of the catalyst is highest for PtAl and Al_2O_3, but when the amount is calculated per surface area, PtTi and TiO_2 take the first positions.

Fig. 3

To find out more information about the type of the acid sites (Lewis acid sites, LAS and Brønsted acid site, BAS), pyridine (Py) and lutidine (Lu) adsorption experiments followed by FTIR were done. The vibration modes and the corresponding wavenumbers used in the determination of Lewis and Brønsted acid sites are summarized in Table 3 taken from the reference [39] for pyridine and from [40] for lutidine. The exact values are depending on the used materials.

Table 3. Wavenumber (cm^{-1}) attribution to different vibration bands coordinated to pyridine (lutidine) versus interaction type, HPy (HLu) is H-bonded pyridine (lutidine), LPy (LLu) and BPy (BLu) mean pyridine (lutidine) coordinated respectively to Lewis acid sites and Brønsted acid sites.

Coordination types	**Vibration modes (cm^{-1})**			
	υ_{19b}	υ_{19a}	υ_{8b}	υ_{8a}

HPy	1440-1445	1480-1490	1577-1580	1580-1600
LPy	1445-1460	1478-1490	1575-1585	1602-1632
BPy	1530-1550	1470-1490	1600-1613	1631-1640
HLu	1410	1480	1580	1600
LLu	1410	1477	1580	1595-1620
BLu	1415	1473	1625-1630	1640-1655

With Py thermo-desorption we were able to observe only the LAS on the studied supports. The Fig. 4 shows the results for γ-Al_2O_3 at selected temperatures. The observed bands at about 1448 (ν_{19b}), 1493 (ν_{19a}), 1577 (ν_{8b}), 1614 and 1621 cm^{-1} (ν_{8a}) are all related to pyridine adsorbed on the LAS [41–43].

Fig. 4

The intensity of the bands decrease when temperature is increased. The band at 1614 cm^{-1} disappears at 350 °C while the band at 1621 cm^{-1} is still visible at 450 °C. These two ν_{8a} bands are assigned to pyridine coordinated to tetrahedral Al^{3+} (1621 cm^{-1}, strong LAS) and to both tetrahedral and octahedral Al^{3+} modes (1614 cm^{-1}, both medium and weak LAS) [43]. The band at 1448 cm^{-1} has a shoulder at 1454 cm^{-1}. After outgassing at 250 °C, the band at 1448 cm^{-1} disappears in accordance to the existence of an H-bond to pyridine and to a weak LAS, while the shoulder at 1454 cm^{-1} remains, which is corresponding to a strong LAS coordinated to pyridine [41]. In a lower temperature range (at room temperature and at 50 °C), a weak band at 1595 cm^{-1} can also be observed indicating hydrogen bonded pyridine [41]. At 450 °C the bands at 1621, 1493 and 1454 cm^{-1} remain, indicating irreversibly held Py/Al on strongly acidic tetrahedrally coordinated Al^{3+} sites. Based on the result γ-Al_2O_3 has all, weak, medium and strong Lewis acid sites on its surface.

We have used earlier in our study Py adsorption in the determination of the Lewis acidity of TiO_2, CeO_2 and MgO and they are discussed in detail in [26]. The total quantity of LAS for all the prepared materials (presented in Fig. 5) was determined based on the ν_{19b} band between 1440 - 1460 cm^{-1} [42] by using the associated molar adsorption coefficient values (ε = 1.28 cm mol^{-1}) [44]. The quantity of strong LAS is determined from the results after evacuation at 300 °C. Table 4 summarizes the amount of weak/medium and strong LAS. When we compare these supports, LAS sites are stronger on γ-Al_2O_3 and TiO_2 than on MgO and CeO_2. This is in accordance with NH_3-TPD. After the Pt impregnation, the same bands detected for the supports were observed for the catalysts with a slight shift of the wavenumbers to higher values and with an increase in the intensity of the bands. This means an increase in the strength and quantity of LAS, which is mainly due to the used acidic Pt precursor and possible presence of residual Cl^- on the catalysts.

Table 4. Number of Lewis acid sites (LAS) as µmol m^{-2}, NT is number of total LAS at 150 °C, NS is number of strong LAS at 300 °C, NWM is number of weak to medium LAS calculated by NT-NS.

	Al_2O_3	PtAl	TiO_2	PtTi	CeO_2	PtCe	MgO	PtMg
NT (µmol m^{-2})	1.25	2.09	2.04	3.13	1.18	1.16	0.03	0.12
NS (µmol m^{-2})	0.54	0.80	0.51	1.06	0.02	0	0	0
NWM (µmol m^{-2})	0.71	1.29	1.53	2.07	1.16	1.16	0.03	0.12

The Fig. 5 represents the amount of Lewis acidity of the samples as a function of temperature. As expected based on the pyridine thermodesorption, only PtAl and Al_2O_3 show the presence of LAS at high temperature. The order of the catalysts based on the total quantity of LAS (µmol m^{-2}) at temperatures above 150 °C and according to Figure 5 is as follows: PtTi > TiO_2 = PtAl > γ-Al_2O_3 > PtCe > CeO_2 > PtMg = MgO.

Fig. 5

To verify the presence or Brønsted acid sites (BAS) the lutidine thermodesorption was studied (results shown in Table 5). First, the results confirmed the presence of a significant quantity of LAS (a band at around 1617 cm^{-1}). The high amount of LAS was observed for Al_2O_3, TiO_2 and CeO_2. LAS were not observed for CeO_2 after 250 °C and for TiO_2 after 450 °C. With lutidine thermodesorption we did not observe any LAS on MgO. Secondly, we observed a doublet that appeared at 1644 and 1625 cm^{-1} due to ν_{8a} and ν_{8b} vibrations, which is related to lutidine coordinated on BAS. This doublet was observed especially for Al_2O_3 and TiO_2, and calculated amounts show that TiO_2 has more and stronger BAS on its surface than Al_2O_3.

Table 5. Evolution of supports acidity (µmol m^{-2}), as a function of temperature, determined by thermodesorption of lutidine.

Temperature (°C)		**150**	**200**	**250**	**300**	**350**	**400**	**450**
Al_2O_3 (µmol m^{-2})	LAS	0.16	0.12	0.09	0.05	0.03	0.02	0.01
	BAS	0.05	0.02	0.01	0	0	0	0
TiO_2 (µmol m^{-2})	LAS	0.23	0.20	0.19	0.07	0.07	0.03	0
	BAS	0.24	0.17	0.04	0.04	0	0	0
CeO_2 (µmol m^{-2})	LAS	0.29	0.10	0	0	0	0	0
	BAS	0	0	0	0	0	0	0
MgO (µmol m^{-2})	LAS	0	0	0	0	0	0	0
	BAS	0.03	0	0	0	0	0	0

3.3. Activity tests

Before the actual activity tests, certain preliminary studies were done. The oxidation test without catalyst showed 8% DCM conversion at 500 °C with 3% HCl yield. During this test the formation of by-products was insignificant. The effect of GHSV was tested with γ-Al_2O_3. It was observed that the

light-off temperature increased by 40 °C when the GHSV increased from 143 800 h^{-1} to almost double: 264 500 h^{-1}. The previous studies have shown that the presence of H_2 rich medium (*e.g.* H_2O, toluene) may affect the HCl formation in DCM oxidation [10,17,28]. In connection to γ-Al_2O_3 experiments we observed that presence of H_2O increases the amounts of HCl and CH_2O while the amounts of CH_3Cl and CO are decreased. Based on these results, and earlier reference, the further experiments were done in presence of H_2O. Since the ICP analysis showed a small difference in the Pt amount on different supports, the effect of the Pt loading on DCM oxidation was also verified. The samples with 0.7 wt-% and 1 wt-% of Pt impregnated on γ-Al_2O_3 were prepared and the activity test results showed only a very small difference in the DCM conversion and HCl formation that falls in the experimental error. It means that the small difference in the Pt loadings on the studied supports should not have a significant effect on the results. However, it may affect certain characterizations and it will be discussed later.

Fig. 6 shows the activities of the prepared samples in the DCM oxidation. The oxidation of DCM started at around 250 °C over all the supports and catalysts, except with PtMg and MgO. These latest two samples are able to convert less than 20% of DCM at around 500 °C and it was the maximum conversion reached during the test. Even though the conversion of DCM over MgO or PtMg was very low, we decided to test the effect of GHSV, since for example in Fig. 6 we used only 167 mg of MgO to have the same GHSV with the other experiments. The result was that using 400 mg of MgO did not improve the DCM oxidation result markedly. In a long run the utilisation of MgO as a support in CVOC oxidation is in any case questionable due to the possible formation of $MgCl_2$. For example, Fenelonov *et al.* [45] studied catalytic oxidation of 1-chlorobutane. They observed that the 1-chlorobutane conversion occurs over MgO via two mechanisms: dehydrochlorination of 1-chlorobutane to a mixture of butylenes and topochemical transformation (reaction occurs on the surface of solid) of MgO to $MgCl_2$. In our case, the possibility of formation of $MgCl_2$ was checked by thermodynamic calculations (HSC chemistry) and it was observed that the formation of $MgCl_2$ occurs at low

temperatures followed by $MgCl_2$ decomposition at temperatures higher than 220 °C [24] when using our DCM oxidation conditions, and thus, only MgO should be present.

Fig. 6

Concerning the other samples, our results showed that the DCM conversion was almost complete at 500 °C. The T_{50} and T_{90} (temperature needed for 50% and 90% of DCM conversion) were used in the comparison of the catalysts' performances. The lowest T_{50} for DCM was 345 °C reached over γ-Al_2O_3 and PtAl, followed closely by PtTi with T_{50} of about 360°C. The T_{50} for TiO_2, PtCe and CeO_2 were somewhat higher. At T_{90} the catalysts kept the same order. It can be noted (Fig. 6) that the Pt impregnation has a clear effect on the DCM conversion only in the case of TiO_2 support, since in most the cases the light-off curves with or without Pt overlapped.

It has been reported earlier by Ran *et al.* [46] that the TiO_2 support is deactivated by adsorbed Cl during DCM oxidation and they observed, that RuO_2 improves the stability of TiO_2. Also Cao *et al.* [47] studied the deactivation of TiO_2–based catalysts and they found out that the Cl-induced deactivation is reduced at higher temperatures, but it cannot be completely avoided even after CeO_2 doping. [47] In our case, the improved activity of PtTi compared with TiO_2 may be due to the Cl adsorption or accumulation on the surface of TiO_2, which is decreased after Pt impregnation. To check out this hypothesis, the XPS analysis was done for TiO_2 and PtTi before and after the DCM oxidation test. The XPS spectral region corresponding to Cl2p for both fresh and used samples consists of one peak at around BE = 198.9 eV, which is assigned to the metal chloride. The surface concentration of Cl for used catalysts are higher than for the fresh samples (Table 6). The existence of chlorine in the fresh catalysts is due to the used precursor during the catalyst preparation and it demonstrates that the reduction at 500°C for 2h is not able to remove the residual chlorine entirely from the samples. The

comparison of the adsorption of Cl between used TiO_2 and PtTi shows that the Cl amount is 50% smaller on PtTi than on TiO_2. Thus, it demonstrates that Pt decreases the Cl adsorption on the TiO_2 and may explain the increase in the activity observed in the light-off tests.

Table 6. Atomic percentage of Cl for used and fresh catalysts analysed by XPS.

	PtTi fresh	**PtTi used**	**TiO_2 fresh**	**TiO_2 used**	**PtCe fresh**	**PtCe-used**	**CeO_2 fresh**	**CeO_2 used**
% of Cl	0.18	0.25	0.08	0.23	0.51	1.80	-	2.1
Adsorbed Cl*	-	0.07	-	0.15	-	1.29	-	2.1

* The adsorbed Cl after test is calculated based on subtraction of initial amount of Cl on the fresh sample from the amount obtained after test

As described above, the order of DCM activity of the supports starting with the best one is the following: γ-Al_2O_3 > TiO_2 > CeO_2 > MgO. This ranking does not have clear correlation with the structural and textural properties, since the order of specific surface area (S_{BET}) and pore volume decreased as follows: γ-Al_2O_3 > CeO_2 > TiO_2 > MgO and the approximate average size of crystallites is increasing with the same order (Table 1). To find out more about the effect of the specific surface area, additional alumina samples were tested. Part of the self-prepared γ-Al_2O_3 was calcined at 900 °C for 2 h and as a result θ-Al_2O_3 (observed by XRD) with the specific surface area (SSA) of 118.5 m^2g^{-1} was achieved. In addition, commercial α-Al_2O_3 with 2.5 m^2g^{-1} as S_{BET} was used. The DCM conversion and HCl yield over γ-Al_2O_3 and θ-Al_2O_3 did not have a significant difference even though the S_{BET} decreased. The DCM conversion and HCl yield over α-Al_2O_3 (20% of DCM conversion at 500 °C) were remarkably lower compared to γ-Al_2O_3 and θ-Al_2O_3 (total conversion of DCM at 500 °C). These results show that very low surface area (2.5 m^2g^{-1}) reduces the DCM oxidation activity remarkably, but a difference between 118.5 and 255 m^2g^{-1} does not affect the activity markedly. Very important consideration related to α-Al_2O_3 is also that its acidity based on NH_3-TPD was remarkably lower (0.17

μmol m^{-2}) than that of γ-Al_2O_3 (0.61 μmol m^{-2}) and θ-Al_2O_3 (0.63 μmol m^{-2}), which may also affect the activity of the α-Al_2O_3. The aim of the current test was to reduce the alumina specific surface area closer to the level of the other supports and see if it affects the DCM conversion. Based on the results, we can conclude that the differences between the S_{BET} values of the used supports and catalysts did not affect significantly the DCM conversion in our case.

The H_2-TPR analysis shows no significant reduction of the studied supports except in the case of CeO_2 support. Thus, reducibility cannot explain the order of the activities of the supports in DCM oxidation directly. Of the Pt-impregnated materials, the highest quantity of H_2 consumption at around 200 °C is observed for PtCe, followed by PtMg, while the better activity is observed for PtAl and PtTi. Chen et al. [37] have studied the DCM oxidation over Pt/CeO_2-Al_2O_3 catalysts and they showed that the best activity is achieved via the synergetic effect of surface acidity and reducibility of the catalyst. In our case we did not observe a direct correlation between good reducibility and the DCM conversion, however, since the good reducibility of CeO_2 and PtCe is related to the good oxygen activation ability, we expect finding smaller formation of reaction by-products. A very small H_2 consumption at low temperature range (below 100 °C) was observed for all the catalysts due to weak interaction of Pt with the support oxide. At this region, PtAl and PtTi showed a bit higher consumption of H_2 than PtMg and PtCe, and it may have a relation with good activity, since PtAl and PtTi were more active than the other two in DCM oxidation. However, to verify this, further studies are needed.

When it comes to acidic properties, Pinard *et al*. [11,12] have concluded that DCM hydrolysis occurs on acid sites of catalysts, but they did not specify which type of acidity (weak, medium or strong) is affecting this step of reaction. PtTi and PtAl, that are the most active catalysts, have higher amount of medium strength acid sites on the surface based on NH_3-TPD. However, this result is not inclusive, since one would expect to see the difference also in by-product formation, which is not clear when also PtCe is taken into the consideration. A very small amount of by-products is observed in the

case of PtCe, but this is more likely related to the higher reducibility and good oxygen activation properties of PtCe than its acidic properties.

The main chlorinated product observed during the light-off tests is HCl. Fig. 7 shows the yields of HCl, which is the desired final chlorinated product in our case (in engineering point of view, the post-treatment of HCl is straight forward). The impregnation of Pt on the support is affecting the HCl yield especially in the case of γ-Al_2O_3. The increase in the HCl yield at higher temperatures might be also due to the release of adsorbed or accumulated Cl species from the surface and the presence of H_2O that give rise to the HCl formation. In the cases of PtCe and CeO_2 the HCl yields observed were very similar. This may be due to very good reducibility and oxygen activation behaviour of CeO_2 that was not significantly improved after the addition of 0.6 wt-% of Pt. If we observe the HCl yields of each material at constant 90% conversion, the result is the following: TiO_2 and PtTi show higher HCl yields (69 and 66%, respectively) than PtCe (59%) and CeO_2 (56%) as well as PtAl (58%) and Al_2O_3 (49%). Selectivity to HCl does not seem to have clear correlation with the reducibility of the materials.

Fig. 7

To discuss further the HCl formation on PtCe and CeO_2, certain earlier observations can be highlighted. CeO_2 has been earlier used in HCl oxidation to Cl_2 by Amrute *et al.* [48]. They observed that the Deacon reaction happened even at low inlet concentrations of O_2 with the formation of new crystalline phase $CeCl_3 \cdot 6H_2O$. This phase was not observed with high inlet concentrations of O_2, and the result was the same in our case, i.e. the formation of $CeCl_3 \cdot 6H_2O$ was not observed with XRD. However, we observed a significant decrease in the cerianite peak intensities and it seems that the crystallinity of the material is affected somehow. In the case of HCl yield at lower temperature (325-425°C), the small influence of Pt impregnation on CeO_2, may be explained in a couple of ways: Cl may

be inserted in oxygen vacancies in CeO_2, it may be deposited on the catalyst in a non-crystalline form or it can also be released to atmosphere as Cl_2. Table 6 shows the atomic percentage of Cl, analysed by XPS, over a fresh ceria based catalyst and the same catalyst used in DCM oxidation. For fresh catalysts, we did not observe a peak corresponding to Cl species on CeO_2, but in the case of PtCe a small peak appeared corresponding to metal chloride with atomic percentage of 0.51%. The used catalysts display higher amount of Cl and the adsorbed amount on the surface of used CeO_2 is higher than on PtCe. The atomic ratio of Cl/Pt and Cl/Ce, between fresh and used PtCe, is increased by 22 and 61 %, respectively. Based on the XPS results, we expect that accumulation and adsorption of Cl on the catalyst surface take place in our case and especially on CeO_2.

In general, the by-products observed during the activity tests were CH_3Cl, CH_2O and CO. The addition of Pt on the support decreases the by-products formation markedly and their amounts become insignificant or they disappear completely at around 500 °C. Pt is improving the total oxidation of DCM, since after Pt impregnation also the CO formation is significantly decreased. One general notice is that CeO_2, which is a good oxygen activator and has important oxygen storage capacity, shows less formation of by-products than the other active supports. Fig. 8 shows the amounts of by-products formed during the tests over the catalysts. The alumina based catalyst had the best activity in DCM oxidation, but PtTi seems to be slightly more selective when the total concentration of reaction products is considered over the whole temperature range.

Fig. 8

The same by-products (CH_2O, CH_3Cl, CO) were also observed by Pinard *et al.* [11,12] during DCM oxidation over NaY, PtNaY, $PtSiO_2$ and HFAU based catalysts. They suggested that CH_2O is produced when the support has the Brønsted acidity and CH_3Cl is produced when the Lewis acidity is present.

Then, these by-products are converted to HCl and CO_2 on the platinum sites. The same result was also obtained when using powder based catalysts (Pt/Al_2O_3) by Maupin *et al*. [13] and by Wang *et al.* [17] by using a platinum catalyst supported on anodic alumite plate. These results are consistent with our results. Furthermore, we observed higher formation of CH_2O on TiO_2 that has more Brønsted sites and higher formation of CH_3Cl on Al_2O_3 that has higher amount of Lewis sites in the sample (when the calculation is done by μmol g^{-1}, because we used the same mass of catalysts in the reaction). The addition of water in the reaction mixture has an effect on the product distribution. We have earlier studied the effect of water on the DCM oxidation activity and HCl yield over a Pt/Al_2O_3 catalyst [10]. With a lower water content (0.5%) the formation of CH_3Cl is higher and decreases during the increase in the water content (maximum tested was 3%). Similarly the formation of CH_2O is decreased, but quantitatively less, and with the water content higher than 1.5%, it starts to be a more important by-product than CH_3Cl. The DCM conversion is not affected by the quantity of water, while HCl production is slightly increased up to 1.5% water content. Assuming the formation of the by-products is related to the quantity of the Brønsted and Lewis acid sites on Pt/Al_2O_3, we would expect a decrease in the Lewis acid sites while increasing the water content and only a slight modification of the Brønsted sites that are responsible for the CH_2O formation. Interestingly it has been also reported that the hydrothermal treatment increases the Lewis acidity of alumina [49], which is opposite to our results, but of course hydrothermal treatment conditions are not the same than oxidation in the presence of water vapor.

The chlorine molar balance was evaluated based on the light-off experiments. We could observe that at 500 °C all the chlorine in reacted DCM is not oxidized to chlorinated products (Fig. 9). It is possible that DCM is also converted to chlorine gas (not detected by FTIR) directly from DCM or according to the Deacon reaction from HCl, however, the Deacon reaction is directed to HCl by adding water to the reaction mixture. Fig. 9 shows the most significant deviation in the chlorine balance on ceria-

containing catalysts. It is good to keep in mind, that in the case of CeO_2 we also observed less (detectable) chlorinated by-products. Amrute *et al.* [48] made a study where they found that CeO_2 is a good catalyst for HCl oxidation to Cl_2. These results make us to consider the possibility of Cl_2 formation during the reaction. Unfortunately, we were not able to confirm this with the current experimental facilities.

Fig. 9

3.4. Durability test

High activity and selectivity are not the only properties needed to prepare the most optimal catalyst for industrial applications. A long operating life and stability are also needed. The most active catalyst from the group of samples, *i.e.* PtAl, was chosen for the durability test.

Fig. 10 show the comparison of DCM conversion and HCl formation over the PtAl catalysts before and after the 55 h durability tests at 400°C. As can be seen, there is no decrease in the activity after 55 h of testing, which is valid also for the HCl formation. The by-products observed are CO, CH_3Cl and CH_2O and the maximum amount is obtained at around 350 °C. The by-products have completely disappeared at 500 °C in both cases. Since water was used in the reaction to improve the selectivity, hydrothermal changes in the PtAl catalyst are basically possible. It has been reported previously, that γ-Al_2O_3 transformation to bohemite occurs at 350°C under hydrothermal conditions [49]. The XRD analysis of the PtAl catalyst after 55h time-on-stream did not show the presence of boehmite nor other structural changes indicating sintering nor the presence of chlorine containing compounds. TEM images before and after the 55 h test (Fig. 2) show an increase in the Pt particle size, which indicates slight sintering of Pt. However, the activity remains the same, which shows also that a change in Pt

particle size from around 1 nm to about 10 nm does not affect the DCM conversion significantly. We have speculated earlier the possibility of the Pt particle size effect on the selectivity of the catalysts. When we compare by-product formation (CO, CH_2O and CH_3Cl) during the light-off tests before and after 55 h stability test in more detail we observed slightly increased formation of CH_2O and CH_3Cl. However, since the difference is less than 10 ppm, we need to make further experiments to clarify this issue. We evaluated also the carbon balance for the first 30 min time-on-stream and for the last 30 min time-on-stream. As a result we found out that the carbon balance was not completely fulfilled and the difference was increased slightly for the last 30 time-on-stream. This may indicate minor changes in the catalyst performance. The NH_3-TPD done for the spent catalyst shows a significant decrease in the total acidity of the catalyst. The acidity decreased to about a half of the original value. This is interesting since DCM conversion was not affected as mentioned before. Clearly more studies should be devoted to the current topic to obtain more information on the catalyst properties and activity-selectivity-stability relationships in DCM oxidation.

Fig. 10

4. Conclusion

In this study, four different catalyst support materials (Al_2O_3, TiO_2, CeO_2 and MgO) were investigated aiming at to find information on their performance in the catalytic oxidation of DCM. The supports were prepared by the sol-gel method, followed by wet impregnation of Pt and characterized with several physico-chemical techniques (TGA, XRD, TPR, XPS, TEM, ICP, N_2 physisorption, NH_3-TPD, lutidine and pyridine thermo-desorption).

The most active and selective catalyst was found to be Pt/Al_2O_3 followed by Pt/TiO_2 and Pt/CeO_2. Pt/MgO did not show any interesting activity in DCM oxidation. Considering the reaction by-products observed during the whole light-off temperature range, the most selective catalyst was Pt/CeO_2 most probably due to its easy reducibility and good oxygen activation ability. Our results support the earlier findings where it is suggested that the DCM reaction first occurs on the acid sites of the support and then the reaction proceeds on the Pt sites to complete oxidation products. The results showed that the existence of Lewis acid sites leads to the formation of CH_3Cl as a by-product while the Brønsted acid sites form CH_2O. The role of acidity properties seem to be more important than reduction behaviour of the catalysts in DCM conversion. Furthermore, the role of the specific surface area and crystallite size of the supports was not that significant, as far as they are at an adequate level.

Pt impregnation (0.5 wt-%) did not have significant effect on the DCM conversions, but it had a major effect on the products' distribution and formation, which supports the earlier presented suggestion for DCM oxidation mechanism. This result was valid with alumina and titania supported catalysts and less pronounced in the case of ceria. It is known that both Pt and ceria have very good oxidation properties, which may explain why the difference between ceria and Pt/CeO_2 was very small in terms of HCl production.

The TEM analysis showed the presence of small Pt particles that were at higher quantity on Al_2O_3 and TiO_2. The small Pt particle size may improve the selectivity of the catalysts, since the final formation of total oxidation products occur on Pt sites. However, more evidence is needed to confirm this result. The most active catalyst, i.e. Pt/Al_2O_3, showed excellent durability based on the chlorine-balance calculation and the longer-term testing, however the Pt particulate size was increased and the total acidity decreased after the test, which may later lead to changes in the catalyst performance.

Acknowledgments

The authors are grateful to Sandrine Arrii-Clacens, Stéphane Pronier, and Jorma Penttinen for their help during the characterization of the catalysts. Esa Turpeinen and Prof. Charles Kappenstein are acknowledged for the thermodynamic calculations.

The work was done with the financial support from PHC Volubilis (N° 24618ZJ) and the Thule Institute at the University of Oulu.

References

[1] EPA, Toxicological review of dichloromethane, EPA. (2011). doi:http://www.epa.gov/iris/toxreviews/0070tr.pdf. (Accessed March 10, 2014)

[2] V.I. Krausova, F.T. Robb, J.M. González, Biodegradation of Dichloromethane in an Estuarine Environment, Hydrobiologia. 559 (2006) 77–83.

[3] Eurochlor, Dichloromethane, (1999). http://www.eurochlor.org/media/14132/dcm.pdf (accessed March 10, 2014).

[4] CDC, Dichloromethane, International Chemical Safety Cards (ICSC), http://www.cdc.gov/niosh/ipcsneng/neng0058.html. (Accessed March 10, 2014)

[5] SCOEL, Recommendation from the Scientific Committee on Occupational Exposure Limits for Acrylamide, 2009. doi:ec.europa.eu/social/BlobServlet?docId=3803&langId=en. (Accessed March 10, 2014)

[6] J.R. González-Velasco, A. Aranzabal, J.I. Gutiérrez-Ortiz, R. López-Fonseca, M.. Gutiérrez-Ortiz, Activity and product distribution of alumina supported platinum and palladium catalysts in the gas-phase oxidative decomposition of chlorinated hydrocarbons, Appl. Catal. B Environ. 19 (1998) 189–197.

[7] J.R. González-Velasco, A. Aranzabal, R. López-Fonseca, R. Ferret, J.A. González-Marcos, Enhancement of the catalytic oxidation of hydrogen-lean chlorinated VOCs in the presence of hydrogen-supplying compounds, Appl. Catal. B Environ. 24 (2000) 33–43.

[8] A.M. Padilla, J. Corella, J.M. Toledo, Total oxidation of some chlorinated hydrocarbons with commercial chromia based catalysts, Appl. Catal. B Environ. 22 (1999) 107–121.

[9] J. Corella, J.M. Toledo, A.M. Padilla, On the selection of the catalyst among the commercial platinum-based ones for total oxidation of some chlorinated hydrocarbons, Appl. Catal. B Environ. 27 (2000) 243–256.

[10] S. Pitkäaho, T. Nevanperä, L. Matejova, S. Ojala, R.L. Keiski, Oxidation of dichloromethane over Pt, Pd, Rh, and V_2O_5 catalysts supported on Al_2O_3, Al_2O_3–TiO_2 and Al_2O_3–CeO_2, Appl. Catal. B Environ. 138-139 (2013) 33–42.

[11] L. Pinard, J. Mijoin, P. Magnoux, M. Guisnet, Oxidation of chlorinated hydrocarbons over Pt zeolite catalysts 1-mechanism of dichloromethane transformation over PtNaY catalysts, J. Catal. 215 (2003) 234–244.

[12] L. Pinard, J. Mijoin, P. Ayrault, C. Canaff, P. Magnoux, On the mechanism of the catalytic destruction of dichloromethane over Pt zeolite catalysts, Appl. Catal. B Environ. 51 (2004) 1–8.

[13] I. Maupin, L. Pinard, J. Mijoin, P. Magnoux, Bifunctional mechanism of dichloromethane oxidation over Pt/Al_2O_3: CH_2Cl_2 disproportionation over alumina and oxidation over platinum, J. Catal. 291 (2012) 104–109.

[14] S. Pitkäaho, S. Ojala, T. Maunula, A. Savimäki, T. Kinnunen, R.L. Keiski, Oxidation of dichloromethane and perchloroethylene as single compounds and in mixtures, Appl. Catal. B Environ. 102 (2011) 395–403.

[15] A. Koyer-Gołkowska, A. Musialik-Piotrowska, J.D. Rutkowski, Oxidation of chlorinated hydrocarbons over Pt–Pd-based catalyst. Part 1. Chlorinated methanes, Catal. Today. 90 (2004) 133–138.

[16] R.W. Van Den Brink, P. Mulder, R. Louw, G. Sinquin, C. Petit, J. Hindermann, Catalytic Oxidation of Dichloromethane on γ-Al_2O_3 : A Combined Flow and Infrared Spectroscopic Study, J. Catal. 180 (1998) 153–160.

[17] L. Wang, M. Sakurai, H. Kameyama, Catalytic oxidation of dichloromethane and toluene over platinum alumite catalyst, J. Hazard. Mater. 154 (2008) 390–395.

[18] U. Weiss, M.P. Rosynek, J. Lunsford, The catalytic hydrolysis of CCl_4 to HCl and CO_2 over magnesium oxide, Chem. Commun. (2000) 405–406.

[19] L. Matějová, P. Topka, L. Kaluža, S. Pitkäaho, S. Ojala, J. Gaálová, R. L. Keiski, Total oxidation of dichloromethane and ethanol over ceria–zirconia mixed oxide supported platinum and gold catalysts, Appl. Catal. B Environ. 142-143 (2013) 54–64.

[20] P. Yang, Z. Shi, S. Yang, R. Zhou, High catalytic performances of CeO_2–CrO_x catalysts for chlorinated VOCs elimination, Chem. Eng. Sci. 126 (2015) 361–369.

[21] J.I. Gutiérrez-Ortiz, B. de Rivas, R. López-Fonseca, J.R. González-Velasco, Combustion of aliphatic C2 chlorohydrocarbons over ceria–zirconia mixed oxides catalysts, Appl. Catal. A Gen. 269 (2004) 147–155.

[22] V.H. Vu, J. Belkouch, A. Ould-Dris, B. Taouk, Removal of hazardous chlorinated VOCs over Mn-Cu mixed oxide based catalyst, J. Hazard. Mater. 169 (2009) 758–765.

[23] B.E. Yoldas, Alumina gels that form porous transparent Al_2O_3, J. Mater. Sci. 10 (1975) 1856–1860.

[24] Z. El Assal, S. Pitkäaho, S. Ojala, R. Maache, M. Bensitel, L. Pirault-Roy, R. Brahmi, R. L. Keiski, Total Oxidation of Dichloromethane Over Metal Oxide Catalysts, Top. Catal. 56 (2013) 679–687.

[25] L. Qiu, F. Liu, L. Zhao, Y. Ma, J. Yao, Comparative XPS study of surface reduction for nanocrystalline and microcrystalline ceria powder, Appl. Surf. Sci. 252 (2006) 4931–4935.

[26] C. Morterra, G. Magnacca, A case study: surface chemistry and surface structure of catalytic aluminas, as studied by vibrational spectroscopy of adsorbed species, Catal. Today. 27 (1996) 497–532.

[27] T. Onfroy, G. Clet, M. Houalla, Quantitative IR characterization of the acidity of various oxide catalysts, Microporous Mesoporous Mater. 82 (2005) 99–104.

[28] S. Pitkäaho, L. Matejova, S. Ojala, J. Gaalova, R.L. Keiski, Oxidation of perchloroethylene—Activity and selectivity of Pt, Pd, Rh, and V_2O_5 catalysts supported on Al_2O_3, Al_2O_3-TiO_2, Appl. Catal. B Environ. 113-114 (2012) 150–159.

[29] M. Thommes, Physical Adsorption Characterization of Nanoporous Materials, Chemie Ing. Tech. 82 (2010) 1059–1073.

[30] M.S. Avila, C.I. Vignatti, C.R. Apesteguía, T.F. Garetto, Effect of support on the deep oxidation of propane and propylene on Pt-based catalysts, Chem. Eng. J. 241 (2014) 52–59.

[31] N. Barrabés, K. Föttinger, A. Dafinov, F. Medina, G. Rupprechter, J. Llorca, J. E. Sueiras, Study of Pt–CeO_2 interaction and the effect in the selective hydrodechlorination of trichloroethylene, Appl. Catal. B Environ. 87 (2009) 84–91.

[32] H.-H. Liu, Y. Wang, A.-P. Jia, S.-Y. Wang, M.-F. Luo, J.-Q. Lu, Oxygen vacancy promoted CO oxidation over Pt/CeO_2 catalysts: A reaction at Pt–CeO_2 interface, Appl. Surf. Sci. 314 (2014) 725–734.

[33] H.C. Yao, Y.F.Y. Yao, Ceria in automotive exhaust catalysts: {I.} Oxygen storage, J. Catal. 86 (1984) 254–265.

[34] M. A Aramendia, J. A Benitez, V. Borau, C. Jimenez, J.M. Marinas, J.R. Ruiz, F. Urbano, Study of MgO and Pt/MgO systems by XRD, TPR, and H-1 MAS NMR, Langmuir. 15 (1999) 1192–1197.

[35] E. Merlen, P. Beccat, J.C. Bertolini, P. Delichère, N. Zanier, B. Didillon, Characterization of Bimetallic Pt–Sn/ Al_2O_3 Catalysts : Relationship between Particle Size and Structure, J. Catal. 159 (1996) 178–188.

[36] P. Reyes, G. Pecchi, M. Morales, J.L.G. Fierro, The nature of the support and the metal precursor on the resistance to sulphur poisoning of Pt supported catalysts, Appl. Catal. A Gen. 163 (1997) 145–152.

[37] Q.-Y. Chen, N. Li, M.-F. Luo, J.-Q. Lu, Catalytic oxidation of dichloromethane over Pt/CeO_2–Al_2O_3 catalysts, Appl. Catal. B Environ. 127 (2012) 159–166.

[38] C.-P. Hwang, C.-T. Yeh, Platinum-oxide species formed by oxidation of platinum crystallites supported on alumina, J. Mol. Catal. A Chem. 112 (1996) 295–302.

[39] M.I. Zaki, M.A. Hasan, F.A. Al-Sagheer, L. Pasupulety, Surface chemistry of acetone on metal oxides : IR observation of acetone adsorption and consequent surface reactions on silica-alumina versus silica and alumina, Langmuir. (2000) 430–436.

[40] L. Oliviero, A. Vimont, J.-C. Lavalley, F. Romero Sarria, M. Gaillard, F. Maugé, 2,6-dimethylpyridine as a probe of the strength of Brønsted acid sites: study on zeolites. Application to alumina, Phys. Chem. Chem. Phys. 7 (2005) 1861–1869.

[41] M.I. Zaki, M.A. Hasan, F.A. Al-sagheer, L. Pasupulety, In situ FTIR spectra of pyridine adsorbed on SiO_2 – Al_2O_3, TiO_2, ZrO_2 and CeO_2: general considerations for the identification of acid sites on surfaces of finely divided metal oxides, Colloids Surfaces A Physicochem. Eng. Asp. 190 (2001) 261–274.

[42] S. Scire, C. Crisafulli, R. Maggiore, S. Minicò, S. Galvagno, Effect of the acid – base properties of Pd – Ca/Al_2O_3 catalysts on the selective hydrogenation of phenol to cyclohexanone: FT-IR and TPD characterization, Appl. Surf. Sci. 136 (1998) 311–320.

[43] F. Can, A. Travert, V. Ruaux, J. Gilson, F. Maugé, R. Hu, R. Hu, R. F. Wormsbecher, FCC gasoline sulfur reduction additives: Mechanism and active sites, J. Catal. 249 (2007) 79–92.

[44] M. Guisnet, P. Ayrault, J. Datka, Acid properties of dealuminated Mordenites Studied by IR spectroscopies: 2. Concentration, Acid Strenght and Heterogeneity of OH Groups, Pol. J. Chem. 71 (1997) 1455–1461.

[45] V.B. Fenelonov, M.S. Mel'gunov, I. V Mishakov, R.M. Richards, V. V Chesnokov, A.M. Volodin, K. J. Klabunde, Changes in Texture and Catalytic Activity of Nanocrystalline MgO during Its Transformation to $MgCl_2$ in the Reaction with 1-Chlorobutane, J. Phys. Chem. B. 105 (2001) 3937–3941.

[46] L. Ran, Z. Qin, Z. Wang, X. Wang, Q. Dai, Catalytic decomposition of CH_2Cl_2 over supported Ru catalysts, Catal. Commun. 37 (2013) 5–8.

[47] S. Cao, H. Wang, F. Yu, M. Shi, S. Chen, X. Weng, X. Weng, Y. Liu, Z. Wu, Catalyst performance and mechanism of catalytic combustion of dichloromethane (CH_2Cl_2) over Ce doped TiO_2, J. Colloid Interface Sci. 463 (2016) 233–241.

[48] A.P. Amrute, C. Mondelli, M. Moser, G. Novell-Leruth, N. López, D. Rosenthal, R. Farra, M. E. Schuster, D. Teschner, T. Schmidt, and J. Pérez-Ramírez, Performance, structure, and mechanism of CeO_2 in HCl oxidation to Cl_2, J. Catal. 286 (2012) 287–297.

[49] R. M. Mironenko, O. B. Belskaya, V. P. Talsi, T. I. Gulyaeva, M. O. Kazakov, A. I. Nizovskii, A. V. Kalinkin, V. I. Bukhtiyarov, A. V. Lavrenov, and V. A. Likholobov, Effect of γ-Al_2O_3 hydrothermal treatment on the formation and properties of platinum sites in Pt/γ-Al_2O_3 catalysts, Appl. Catal. A Gen. 469 (2014) 472–482.

Fig. 1 Temperature Programmed Reduction profiles of a) supports (10% H_2/Ar) (Al_2O_3 (Al), TiO_2 (Ti), CeO_2 (Ce) and MgO (Mg)) and b) different Pt based catalysts (1% H_2/Ar).

Fig. 2 TEM images for a) PtAl, b) PtTi, c) PtCe, d) PtMg and e) PtAl after the durability test.

Fig. 3 Temperature Programmed Desorption of ammonia over different catalysts, where range 1 is showing physisorbed NH_3 and weak acid sites, ranges 2 and 3 are medium and strong acid sites, respectively. Grey areas are showing the variation in the reported temperatures for the ranges of acidic strength [66–68].

Fig. 4 FTIR absorbance spectra of pyridine desorption on Al_2O_3 after evacuation at room temperature (RT), 150, 300 and 450 °C.

Fig. 5 The evolution of Lewis acidity amount as a function of temperature over the samples studied where Al, Ti, Ce and Mg are Al_2O_3, TiO_2, CeO_2 and MgO, respectively and LAS is Lewis acid site.

Fig. 6 Activity of the catalysts in the oxidation of DCM where HT is a thermal test, DCM = 500 ppm, H_2O = 1.5 vol-%, m_{cat} = 400 mg (m_{MgO} = 167 mg) and GHSV = 143793 h^{-1} where Al, Ti, Ce and Mg are Al_2O_3, TiO_2, CeO_2 and MgO, respectively.

Fig. 7 HCl formation over the prepared catalysts with same experimental conditions as in Fig. 6.

Fig. 8 Comparison of by-products formation over Al_2O_3 (Al), TiO_2 (Ti) and CeO_2 (Ce) based-catalysts with the same experimental conditions as in Fig. 6.

Fig. 9 Molar balance at 500 °C for chlorine (Cl). Product taken into account in calculation are HCl, CH_3Cl, $CHCl_3$ C_2HCl_3 C_2Cl_4 and $COCl_2$, where Al, Ti and Ce are Al_2O_3, TiO_2 and CeO_2, respectively.

Fig. 10 Comparison of activity and HCl formation over PtAl catalysts in DCM oxidation before (Be) and after (Af) 55 h of durability test, C_{DCM} = 500 ppm, H_2O= 1.5 vol-%, and GHSV= 143 793 h^{-1}.

Figure 1

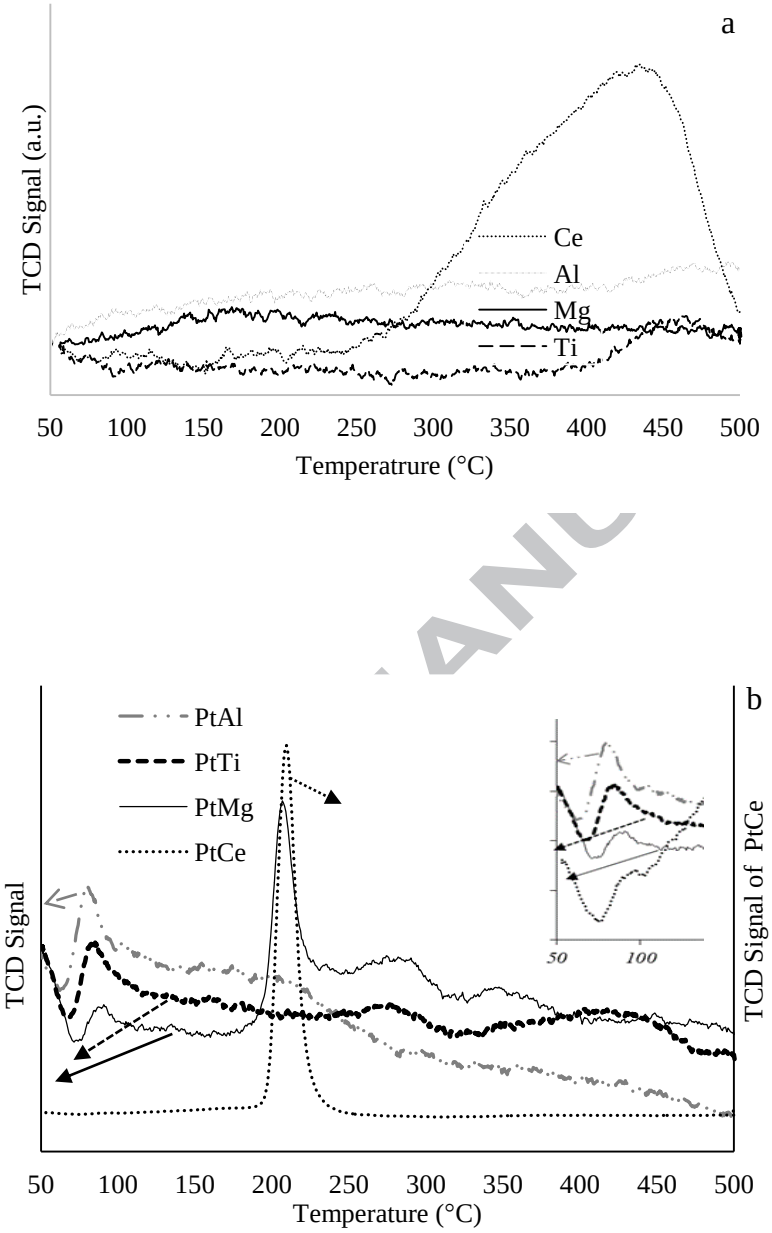

Figure 2

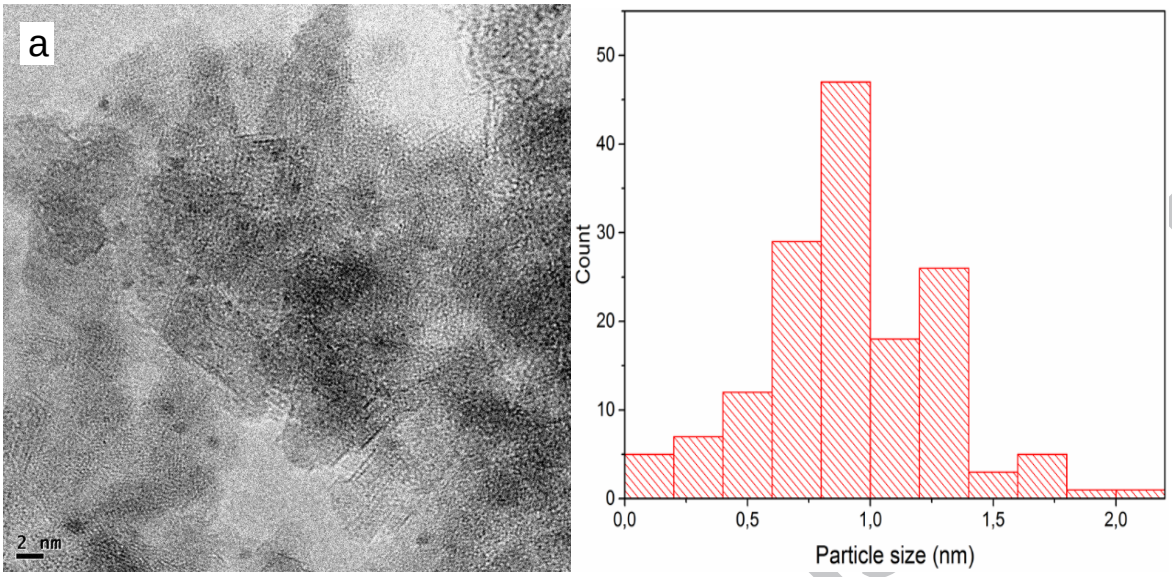

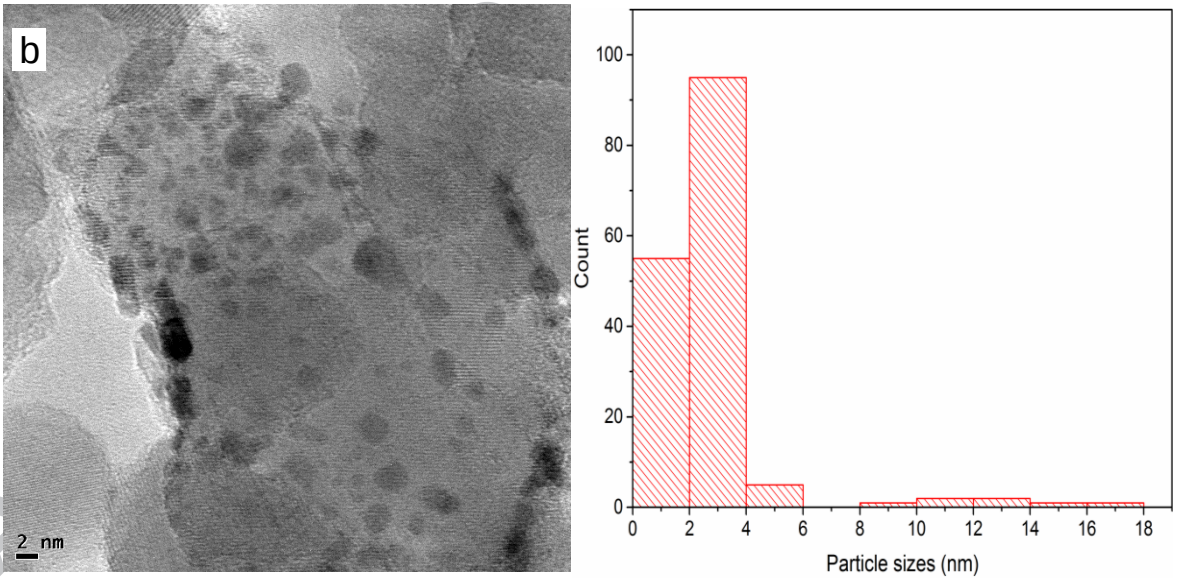

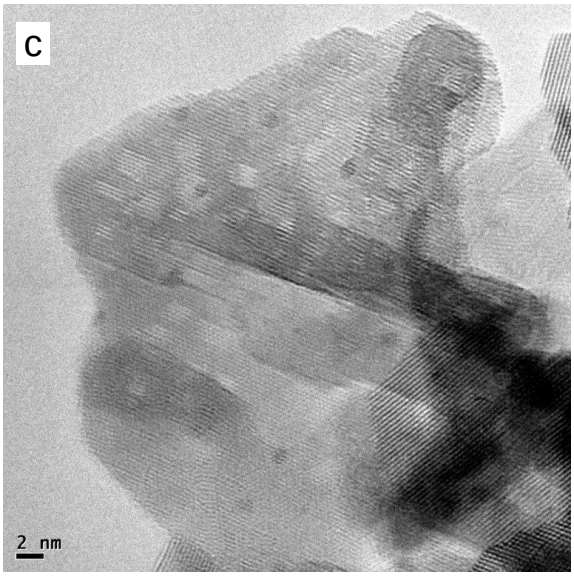

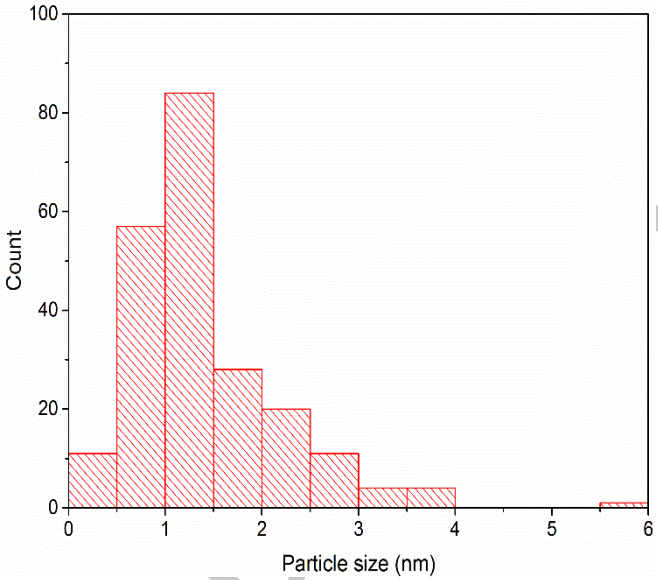

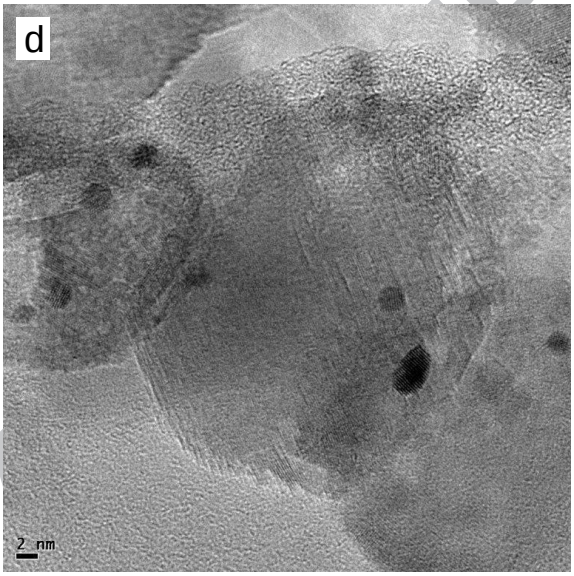

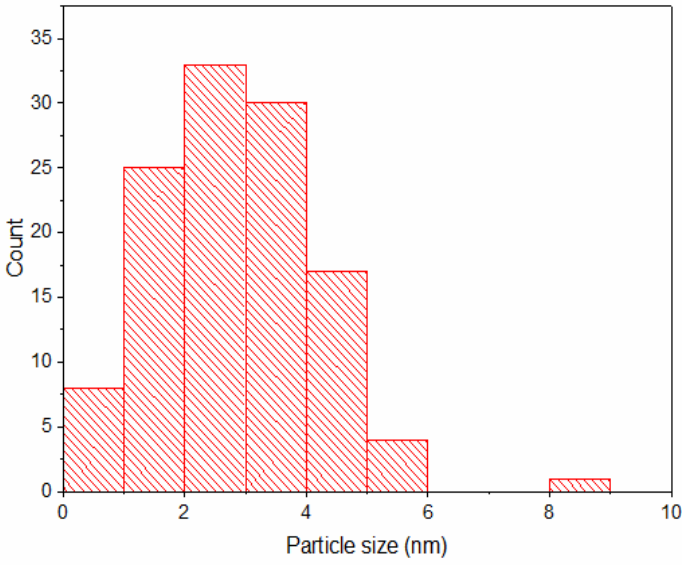

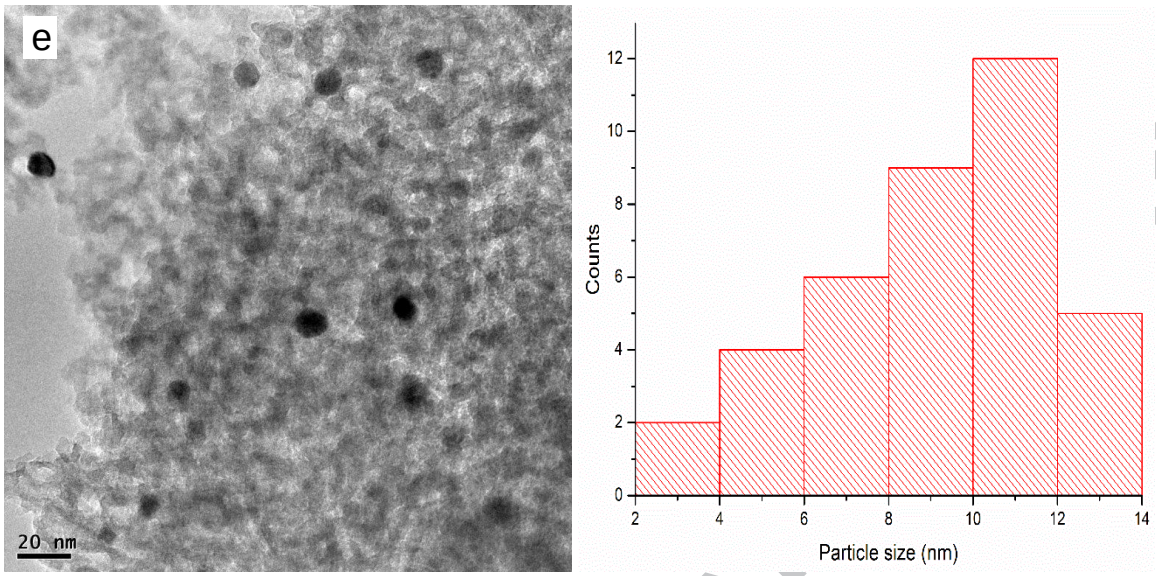

Figure 3

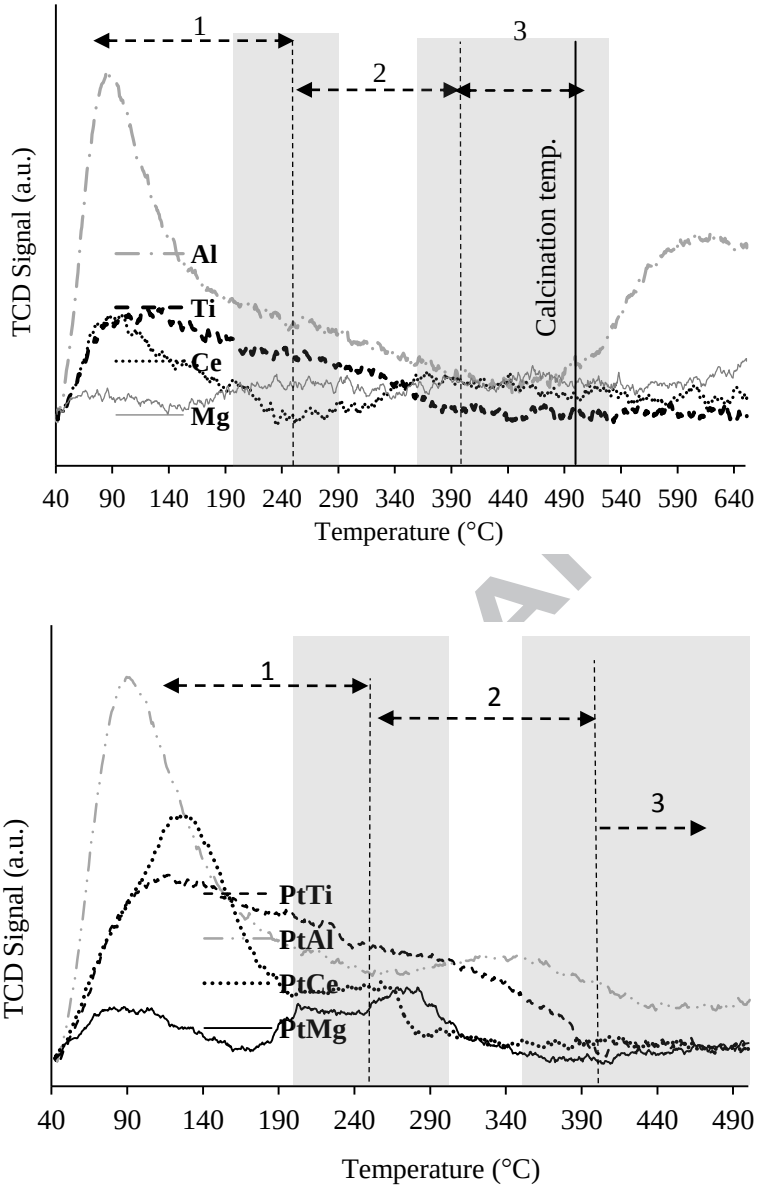

Figure 4

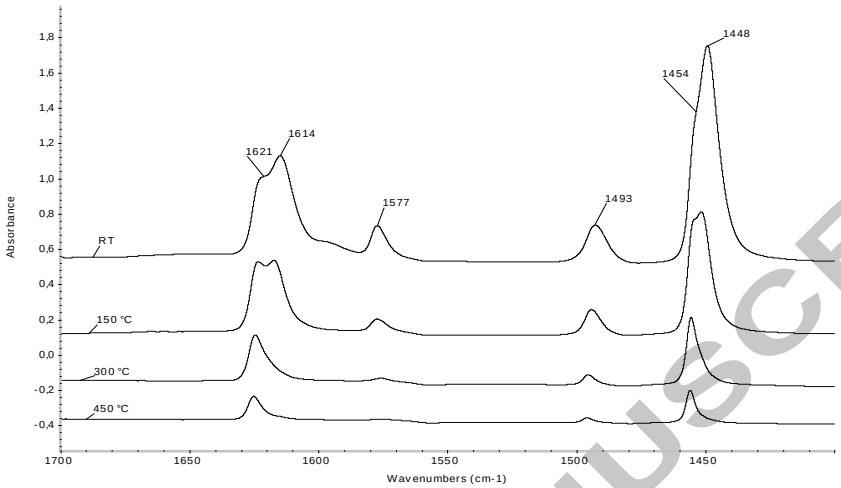

Figure 5

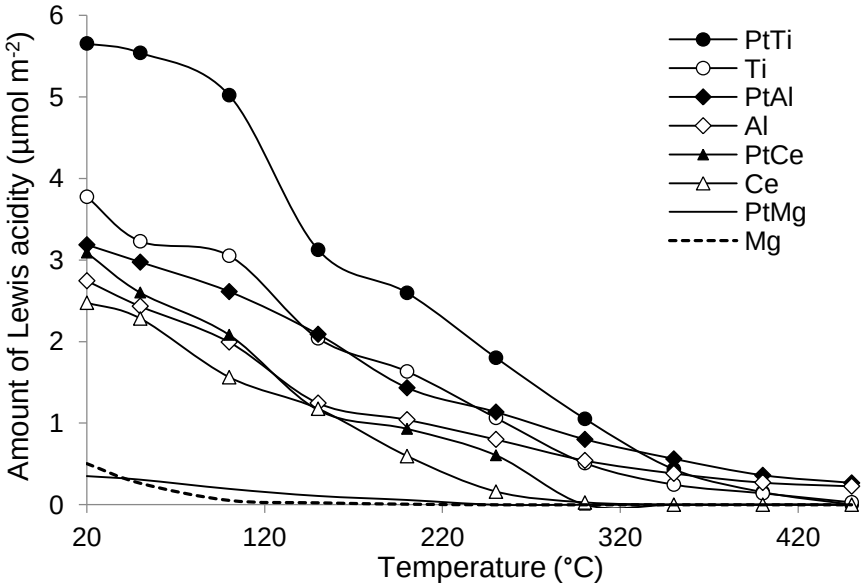

Figure 6

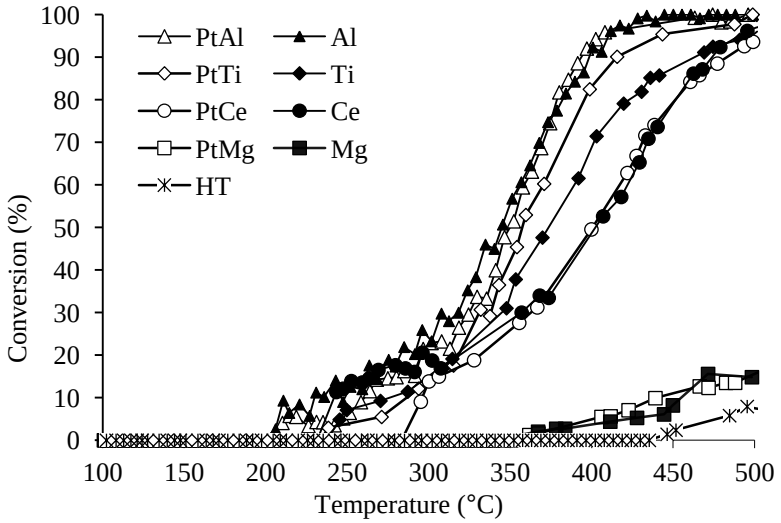

Figure 7

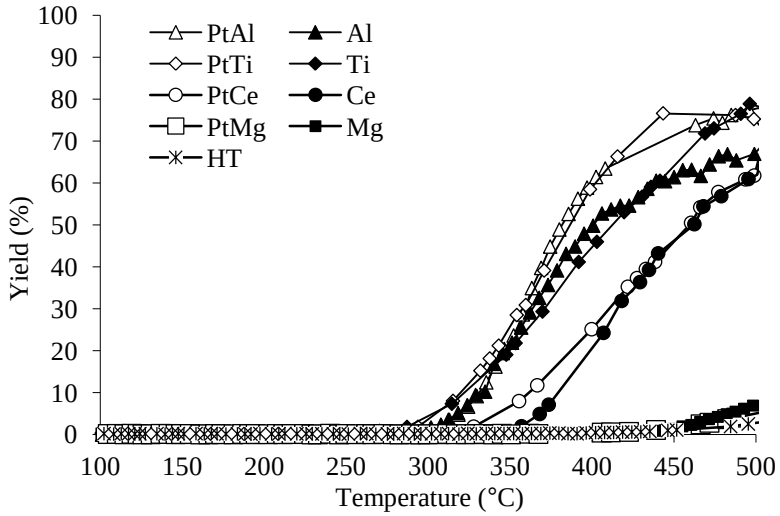

Figure 8

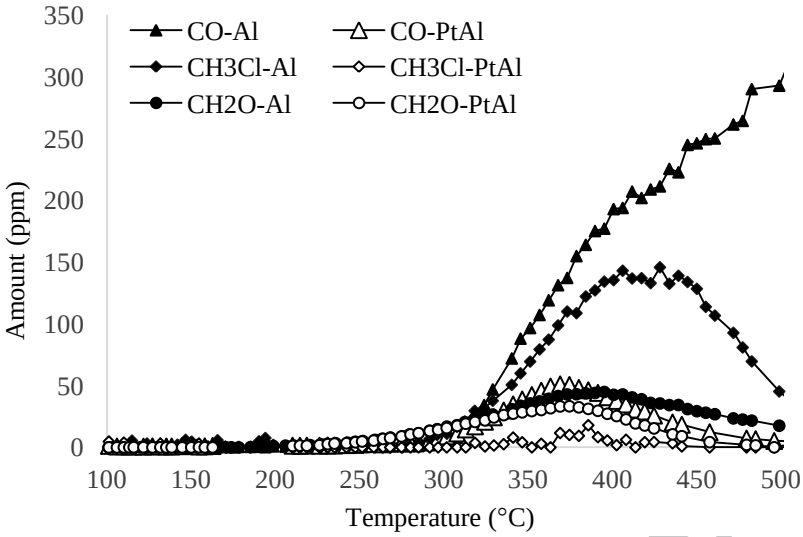

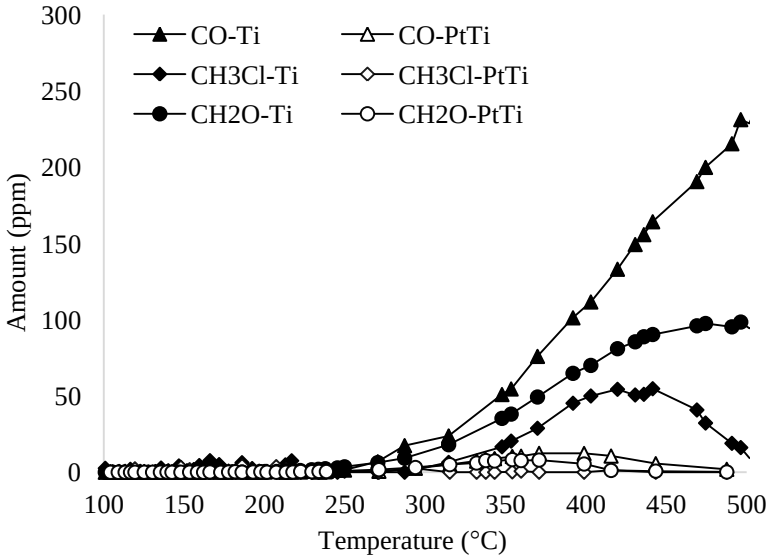

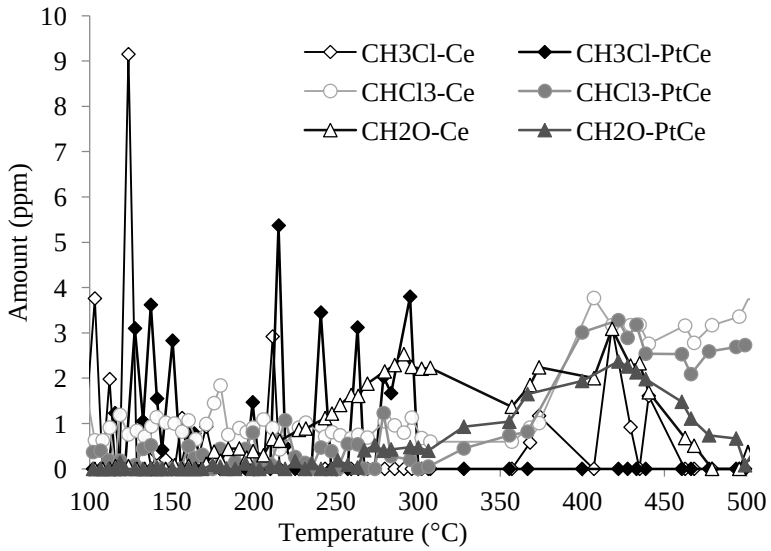

Figure 9

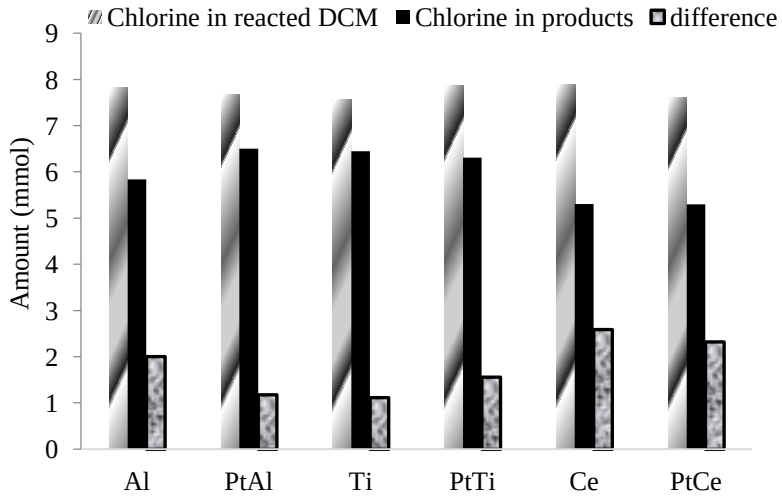

Figure 10

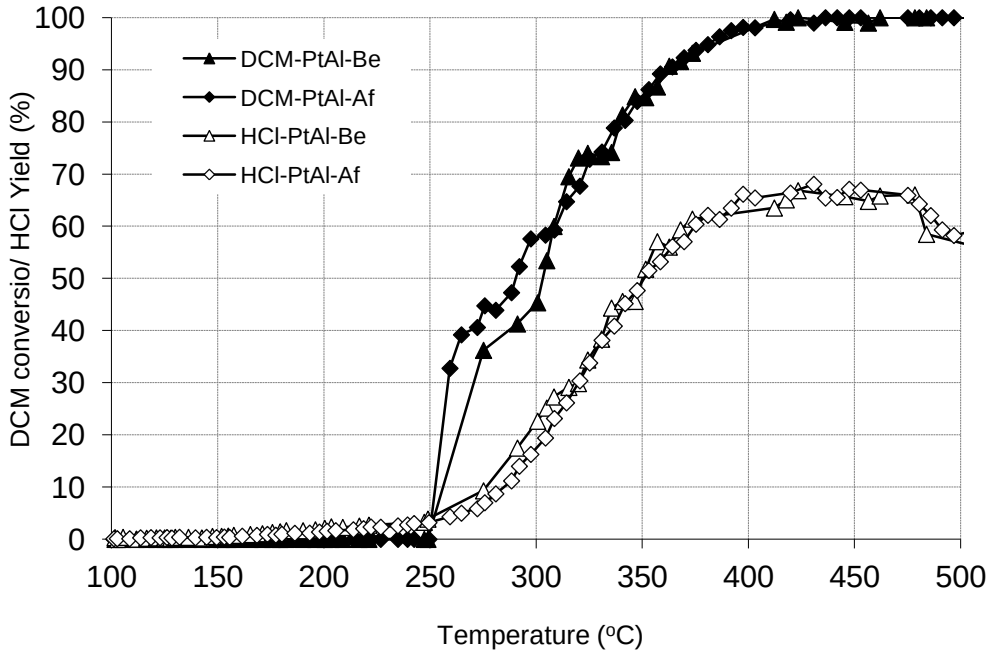

Graphical abstract

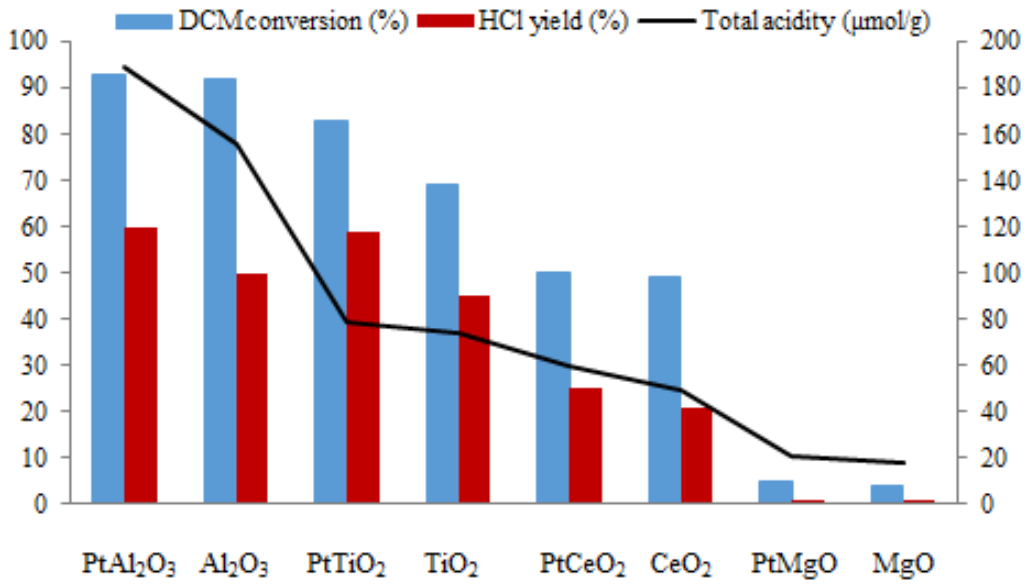

Highlights

- Total conversion of dichloromethane was reached at 450 °C over Al_2O_3 and $PtAl_2O_3$
- Formation of by-products over $PtTiO_2$ and $PtCeO_2$ is smaller than over $PtAl_2O_3$
- Dichloromethane oxidation is influenced by the nature and quantity of acid sites
- By-products formation is influenced by acid sites and catalyst reducibility
- Pt/Al_2O_3 showed good activity even after 55h of stability test